

## Flavour Symmetry and Clean Strategies to Extract $\gamma$

Robert Fleischer

*Theory Division, CERN, CH-1211 Geneva 23, Switzerland*

### Abstract

One of the key elements in the testing of the Standard-Model description of CP violation through  $B$ -meson decays is the direct determination of the angle  $\gamma$  of the unitarity triangle in a variety of ways. We give a brief overview of the implications of the current  $B$ -factory data for flavour-symmetry strategies, and discuss new, theoretically clean methods employing pure tree decays of neutral  $B_{d,s}$  mesons.

*Invited talk at the Workshop on the CKM Unitarity Triangle,  
Durham, United Kingdom, 5–9 April 2003  
To appear in the Proceedings (SLAC eConf service)*





# Flavour Symmetry and Clean Strategies to Extract $\gamma$

R Fleischer

Theory Division, CERN, CH-1211 Geneva 23, Switzerland

One of the key elements in the testing of the Standard-Model description of CP violation through  $B$ -meson decays is the direct determination of the angle  $\gamma$  of the unitarity triangle in a variety of ways. We give a brief overview of the implications of the current  $B$ -factory data for flavour-symmetry strategies, and discuss new, theoretically clean methods employing pure tree decays of neutral  $B_{d,s}$  mesons.

## 1 Introduction

As is well known, the “standard analysis” of the unitarity triangle (UT) allows us to obtain “indirect” ranges for its three angles  $\alpha$ ,  $\beta$  and  $\gamma$  [ 1]. To this end, we apply the Standard Model (SM), and measure the UT side  $R_b \propto |V_{ub}/V_{cb}|$  through semileptonic  $B$  decays caused by  $b \rightarrow u\ell\bar{\nu}_\ell, c\ell\bar{\nu}_\ell$  quark-level transitions, determine the UT side  $R_t \propto |V_{td}/V_{cb}|$  through experimental information on the mass differences  $\Delta M_{d,s}$ , and employ the indirect CP violation in the neutral kaon system, which is described by the famous observable  $\varepsilon_K$ , to calculate a hyperbola in the  $\bar{\rho}-\bar{\eta}$  plane of the generalized Wolfenstein parameters [ 2, 3].

A crucial element in the stringent testing of the Kobayashi–Maskawa mechanism for CP violation is the direct determination of the UT angle  $\gamma$ . Many strategies to accomplish this task were proposed, where also decays of  $B_s$  mesons – the “El Dorado” for hadron colliders – play a prominent rôle (for a detailed review, see [ 4]). The main goal of this programme is to overconstrain  $\gamma$  as much as possible, hoping to encounter inconsistencies.

## 2 Flavour-Symmetry Strategies

A very interesting avenue to determine  $\gamma$  from non-leptonic  $B$  decays is provided by the flavour symmetries of strong interactions. The basic idea is to use isospin or  $SU(3)$  arguments to deal with “unknown” hadronic matrix elements of local four-quark operators. In some cases, also plausible dynamical assumptions have to be made in order to reduce the number of parameters entering the decay amplitudes.

### 2.1 $B \rightarrow \pi K$ Decays

These modes originate from  $\bar{b} \rightarrow \bar{d}\bar{s}, \bar{u}\bar{s}$  quark-level processes, and may receive contributions both from penguin and from tree topologies, where the latter bring  $\gamma$  into the game. Since the ratio of tree to penguin contributions is governed by the tiny CKM factor  $|V_{us}V_{ub}^*/(V_{ts}V_{tb}^*)| \approx 0.02$ ,  $B \rightarrow \pi K$  decays are dominated by QCD penguins, despite

their loop suppression. As far as electroweak (EW) penguins are concerned, their effects are expected to be negligible in the case of the  $B_d^0 \rightarrow \pi^- K^+, B^+ \rightarrow \pi^+ K^0$  system, as they contribute here only in colour-suppressed form. On the other hand, EW penguins may also contribute in colour-allowed form to  $B^+ \rightarrow \pi^0 K^+$  and  $B_d^0 \rightarrow \pi^0 K^0$ , and are hence expected to be sizeable in these modes, i.e. of the same order of magnitude as the tree topologies.

Thanks to interference effects between tree and penguin amplitudes, we obtain sensitivity on  $\gamma$ . In order to determine this angle, we may use an isospin relation as a starting point, suggesting the following combinations: the “mixed”  $B^\pm \rightarrow \pi^\pm K, B_d \rightarrow \pi^\mp K^\pm$  system [ 5]–[ 8], the “charged”  $B^\pm \rightarrow \pi^\pm K, B^\pm \rightarrow \pi^0 K^\pm$  system [ 9]–[ 11], and the “neutral”  $B_d \rightarrow \pi^0 K, B_d \rightarrow \pi^\mp K^\pm$  system [ 11, 12]. As noted in [ 11], all three  $B \rightarrow \pi K$  systems can be described by the same set of formulae by just making straightforward replacements of variables. Let us first focus on the charged and neutral  $B \rightarrow \pi K$  systems. In order to determine  $\gamma$  and the corresponding strong phases, we have to introduce appropriate CP-conserving and CP-violating observables:

$$R_c \equiv 2 \left[ \frac{\text{BR}(B^+ \rightarrow \pi^0 K^+) \pm \text{BR}(B^- \rightarrow \pi^0 K^-)}{\text{BR}(B^+ \rightarrow \pi^+ K^0) + \text{BR}(B^- \rightarrow \pi^- \bar{K}^0)} \right] \quad (1)$$

$$R_n \equiv \frac{1}{2} \left[ \frac{\text{BR}(B_d^0 \rightarrow \pi^- K^+) \pm \text{BR}(\bar{B}_d^0 \rightarrow \pi^+ K^-)}{\text{BR}(B_d^0 \rightarrow \pi^0 K^0) + \text{BR}(\bar{B}_d^0 \rightarrow \pi^0 \bar{K}^0)} \right], \quad (2)$$

where the  $R_{c,n}$  and  $A_0^{c,n}$  refer to the plus and minus signs, respectively. For the parametrization of these observables, we employ the isospin relation mentioned above, and assume that certain rescattering effects are small, which is in accordance with the QCD factorization picture [ 13, 14]; large rescattering processes would be indicated by  $B \rightarrow KK$  modes, which are already strongly constrained by the  $B$  factories, and could be included through more elaborate strategies [ 8, 10, 11]. Following these lines, we may write

$$R_{c,n} = \text{fct}(q, r_{c,n}, \delta_{c,n}, \gamma), \quad A_0^{c,n} = \text{fct}(r_{c,n}, \delta_{c,n}, \gamma), \quad (3)$$

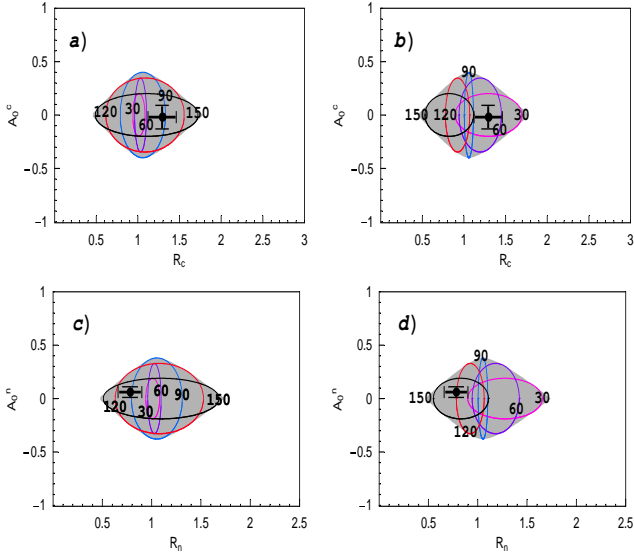


**Figure 1.** The allowed regions in observable space of the charged ( $r_c = 0.20$ ; (a), (b)) and neutral ( $r_n = 0.19$ ; (c), (d))  $B \rightarrow \pi K$  systems for  $q = 0.68$ : in (a) and (c), we show also the contours for fixed values of  $\gamma$ , whereas we give the curves arising for fixed values of  $|\delta_c|$  and  $|\delta_n|$  in (b) and (d), respectively.

where the parameters  $q$ ,  $r_{c,n}$  and  $\delta_{c,n}$  have the following meaning:  $q$  describes the ratio of EW penguin to tree contributions, and can be determined with the help of  $SU(3)$  flavour-symmetry arguments, yielding  $q \sim 0.7$  [9]. On the other hand,  $r_{c,n}$  measures the ratio of tree to QCD penguin topologies, and can be fixed through  $SU(3)$  arguments and data on  $B^\pm \rightarrow \pi^\pm \pi^0$  modes [15], which give  $r_{c,n} \sim 0.2$ . Finally,  $\delta_{c,n}$  is the CP-conserving strong phase between the tree and QCD penguin amplitudes. Since we may fix  $q$  and  $r_{c,n}$ , the observables  $R_{c,n}$  and  $A_0^{c,n}$  actually depend only on the two “unknown” parameters  $\delta_{c,n}$  and  $\gamma$ . If we vary them within their allowed ranges, i.e.  $-180^\circ \leq \delta_{c,n} \leq +180^\circ$  and  $0^\circ \leq \gamma \leq 180^\circ$ , we obtain an allowed region in the  $R_{c,n}$ – $A_0^{c,n}$  plane [16, 17]. Should the measured values of  $R_{c,n}$  and  $A_0^{c,n}$  fall outside this region, we would have an immediate signal for new physics (NP). On the other hand, should the measurements lie inside the allowed range,  $\gamma$  and  $\delta_{c,n}$  could be extracted. The value of  $\gamma$  thus obtained could then be compared with the results of other strategies, whereas the strong phase  $\delta_{c,n}$  would offer interesting insights into hadron dynamics. This exercise can be performed separately for the charged and neutral  $B \rightarrow \pi K$  systems.

In Fig. 1, we show the allowed regions in the  $R_{c,n}$ – $A_0^{c,n}$  planes [17], where the crosses represent the averages of the most recent  $B$ -factory data [18, 19]. As can be read off from the contours in these figures, both the charged and the neutral  $B \rightarrow \pi K$  data favour  $\gamma \gtrsim 90^\circ$ , which would be in conflict with the CKM fits resulting from the “standard analysis” of the UT, favouring

$$50^\circ \leq \gamma \leq 70^\circ. \quad (4)$$

Interestingly, the charged modes point towards  $|\delta_c| \lesssim 90^\circ$  (factorization predicts  $\delta_c$  to be close to  $0^\circ$  [14]), whereas the neutral decays seem to prefer  $|\delta_n| \gtrsim 90^\circ$ . Since we do not expect  $\delta_c$  to differ significantly from  $\delta_n$ , we arrive at a “puzzling” picture of the kind that was already considered a couple of years ago in [12]. Unfortunately, the experimental uncertainties do not yet allow us to draw definite conclusions. As far as the mixed  $B \rightarrow \pi K$  system is concerned, the data fall well into the SM region in observable space, and do not show any “anomalous” behaviour at the moment. For a selection of alternative analyses of  $B \rightarrow \pi K$  decays, see [14, 20, 21, 22, 23].

## 2.2 The $B_d \rightarrow \pi^+ \pi^-$ , $B_s \rightarrow K^+ K^-$ System

The decay  $B_d^0 \rightarrow \pi^+ \pi^-$  originates from  $\bar{b} \rightarrow \bar{u} u \bar{d}$  quark-level processes. Within the SM, its transition amplitude may be written as

$$A(B_d^0 \rightarrow \pi^+ \pi^-) \propto [e^{i\gamma} - d e^{i\theta}], \quad (5)$$

where the CP-conserving strong parameter  $d e^{i\theta}$  measures – sloppily speaking – the ratio of the penguin to tree contributions [24]. As is well known, if we had negligible penguin contributions, i.e.  $d = 0$ , the direct and mixing-induced CP asymmetries provided by the time-dependent rate asymmetry of the kind [4]

$$\frac{\Gamma(B_d^0(t) \rightarrow f) - \Gamma(\bar{B}_d^0(t) \rightarrow f)}{\Gamma(B_d^0(t) \rightarrow f) + \Gamma(\bar{B}_d^0(t) \rightarrow f)} = \left[ \frac{\mathcal{A}_{\text{CP}}^{\text{dir}} \cos(\Delta M_q t) + \mathcal{A}_{\text{CP}}^{\text{mix}} \sin(\Delta M_q t)}{\cosh(\Delta \Gamma_q t/2) - \mathcal{A}_{\Delta \Gamma} \sinh(\Delta \Gamma_q t/2)} \right] \quad (6)$$

were simply given as follows:

$$\mathcal{A}_{\text{CP}}^{\text{dir}}(B_d \rightarrow \pi^+ \pi^-) = 0 \quad (7)$$

$$\mathcal{A}_{\text{CP}}^{\text{mix}}(B_d \rightarrow \pi^+ \pi^-) = \sin(\phi_d + 2\gamma) \stackrel{\text{SM}}{=} -\sin 2\alpha. \quad (8)$$

Here we have used both the SM expression  $\phi_d = 2\beta$  and the unitarity relation  $2\beta + 2\gamma = 2\pi - 2\alpha$  to derive the last identity in (8). We observe that  $\phi_d$  and  $\gamma$  actually enter directly  $\mathcal{A}_{\text{CP}}^{\text{mix}}(B_d \rightarrow \pi^+ \pi^-)$ , and not  $\alpha$ . Consequently, since we may fix  $\phi_d$  straightforwardly through  $B_d \rightarrow J/\psi K_S$ , also if NP should contribute to  $B_d^0$ – $\bar{B}_d^0$  mixing, we may use the CP-violating  $B_d \rightarrow \pi^+ \pi^-$  observables to probe  $\gamma$ . This avenue is of great advantage to deal with penguin effects and possible NP contributions to  $B_d^0$ – $\bar{B}_d^0$  mixing [17, 24, 25].

Measurements of the CP asymmetries of the  $B_d \rightarrow \pi^+ \pi^-$  channel are already available:

$$\mathcal{A}_{\text{CP}}^{\text{dir}} = \begin{cases} -0.30 \pm 0.25 \pm 0.04 & (\text{BaBar [26]}) \\ -0.77 \pm 0.27 \pm 0.08 & (\text{Belle [27]}) \end{cases} \quad (9)$$

$$\mathcal{A}_{\text{CP}}^{\text{mix}} = \begin{cases} -0.02 \pm 0.34 \pm 0.05 & (\text{BaBar [26]}) \\ +1.23 \pm 0.41^{+0.07}_{-0.08} & (\text{Belle [27]}). \end{cases} \quad (10)$$

The BaBar and Belle results are unfortunately not fully consistent with each other. If we form, nevertheless, the weighted averages of (9) and (10), applying the rules of the Particle Data Group (PDG), we obtain

$$\mathcal{A}_{\text{CP}}^{\text{dir}} = -0.51 \pm 0.19 \quad (0.23) \quad (11)$$

$$\mathcal{A}_{\text{CP}}^{\text{mix}} = +0.49 \pm 0.27 \quad (0.61), \quad (12)$$

where the errors in brackets are those increased by the PDG scaling-factor procedure [28]. Direct CP violation at this level would require large penguin contributions, with large CP-conserving strong phases, which are not suggested by the QCD factorization approach, pointing towards  $\mathcal{A}_{\text{CP}}^{\text{dir}}(B_d \rightarrow \pi^+\pi^-) \sim +0.1$  [14]. In addition to (11), a significant impact of penguins on  $B_d \rightarrow \pi^+\pi^-$  is also indicated by the data for the  $B \rightarrow \pi K, \pi\pi$  branching ratios [17, 25], as well as by theoretical considerations [14, 20]. Consequently, it is already evident that we *must* care about the penguin contributions in order to extract information on the UT from the  $B_d \rightarrow \pi^+\pi^-$  CP asymmetries.

In the literature, many approaches to address this challenging problem can be found (see [4] and references therein). Let us focus here on a strategy that complements  $B_d \rightarrow \pi^+\pi^-$  with  $B_s \rightarrow K^+K^-$  [24]. In analogy to (5), the amplitude of the latter decay, which is very accessible at  $B$ -decay experiments at hadron colliders [29]–[31], can be written as follows:

$$A(B_s^0 \rightarrow K^+K^-) \propto \left[ e^{i\gamma} + \left( \frac{1-\lambda^2}{\lambda^2} \right) d' e^{i\theta'} \right], \quad (13)$$

where the hadronic quantities  $d'$  and  $\theta'$  are the  $B_s \rightarrow K^+K^-$  counterparts of the parameters  $d$  and  $\theta$ . Consequently, we obtain observables of the following structure:

$$\begin{aligned} \mathcal{A}_{\text{CP}}^{\text{dir}}(B_d \rightarrow \pi^+\pi^-) &= \text{fct}(d, \theta, \gamma) \\ \mathcal{A}_{\text{CP}}^{\text{mix}}(B_d \rightarrow \pi^+\pi^-) &= \text{fct}(d, \theta, \gamma, \phi_d) \end{aligned} \quad (14)$$

$$\begin{aligned} \mathcal{A}_{\text{CP}}^{\text{dir}}(B_s \rightarrow K^+K^-) &= \text{fct}(d', \theta', \gamma) \\ \mathcal{A}_{\text{CP}}^{\text{mix}}(B_s \rightarrow K^+K^-) &= \text{fct}(d', \theta', \gamma, \phi_s), \end{aligned} \quad (15)$$

where  $\phi_d$  and  $\phi_s$  entering the mixing-induced CP asymmetries can straightforwardly be fixed separately [4], also if NP should contribute to  $B_q^0 - \bar{B}_q^0$  mixing ( $q \in \{d, s\}$ ). We may then use the  $B_d \rightarrow \pi^+\pi^-$  observables to eliminate the strong phase  $\theta$ , which allows us to determine  $d$  as a function of  $\gamma$  in a *theoretically clean* manner, i.e. without using flavour symmetry or plausible dynamical assumptions. Analogously, we may employ the  $B_s \rightarrow K^+K^-$  CP asymmetries to eliminate  $\theta'$ , yielding  $d'$  as a *theoretically clean* function of  $\gamma$ . If we have a look at the corresponding

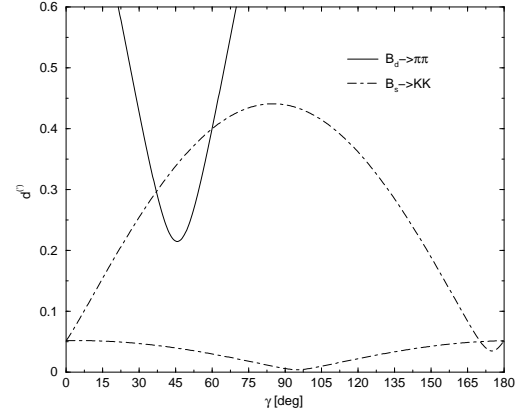


**Figure 2.** The  $\gamma$ - $d^{(\prime)}$  contours for an example with  $d = d' = 0.4$ ,  $\theta = \theta' = 140^\circ$ ,  $\phi_d = 47^\circ$ ,  $\phi_s = 0^\circ$ ,  $\gamma = 60^\circ$ , corresponding to  $\mathcal{A}_{\text{CP}}^{\text{dir}}(B_d \rightarrow \pi^+\pi^-) = -0.30$ ,  $\mathcal{A}_{\text{CP}}^{\text{mix}}(B_d \rightarrow \pi^+\pi^-) = +0.63$ ,  $\mathcal{A}_{\text{CP}}^{\text{dir}}(B_s \rightarrow K^+K^-) = +0.16$  and  $\mathcal{A}_{\text{CP}}^{\text{mix}}(B_s \rightarrow K^+K^-) = -0.17$ .

Feynman diagrams, we observe that  $B_d \rightarrow \pi^+\pi^-$  is related to  $B_s \rightarrow K^+K^-$  through an interchange of all down and strange quarks. Consequently, the  $U$ -spin flavour symmetry of strong interactions implies

$$d' = d, \quad \theta' = \theta. \quad (16)$$

If we now apply the former relation, we may determine  $\gamma$  and  $d$  from the theoretically clean contours in the  $\gamma$ - $d$  and  $\gamma$ - $d'$  planes, as well as the strong phases  $\theta'$  and  $\theta$ , which provide a nice consistency check of the latter  $U$ -spin relation [24]. In Fig. 2, we have illustrated these contours for a specific example.

This strategy is very promising from an experimental point of view: at run II of the Tevatron and the LHC, experimental accuracies for  $\gamma$  of  $O(10^\circ)$  and  $O(1^\circ)$ , respectively, are expected [29, 30]. As far as  $U$ -spin-breaking corrections to  $d' = d$  are concerned [24, 32], they enter the determination of  $\gamma$  through a relative shift of the  $\gamma$ - $d$  and  $\gamma$ - $d'$  contours; their impact on the extracted value of  $\gamma$  depends on the form of these curves, which is fixed through the measured observables. In the examples discussed in [4, 24], as well as in the one shown in Fig. 2, the extracted value of  $\gamma$  would be very robust under such corrections.

Since  $B_s \rightarrow K^+K^-$  is not accessible at the  $\Upsilon(4S)$   $e^+e^-$   $B$  factories, we may not yet implement this strategy. However,  $B_s \rightarrow K^+K^-$  is related to  $B_d \rightarrow \pi^\mp K^\pm$  through an interchange of spectator quarks. Consequently, we may approximately replace  $B_s \rightarrow K^+K^-$  through  $B_d \rightarrow \pi^\mp K^\pm$  to deal with the penguin problem in  $B_d \rightarrow \pi^+\pi^-$  [25]. The utility of  $B_d \rightarrow \pi^\mp K^\pm$  decays to control the penguin effects in  $B_d \rightarrow \pi^+\pi^-$  was also emphasized in [33]. In order to explore the implications of the  $B$ -factory data, the following quantity, which involves the ratio of the corresponding

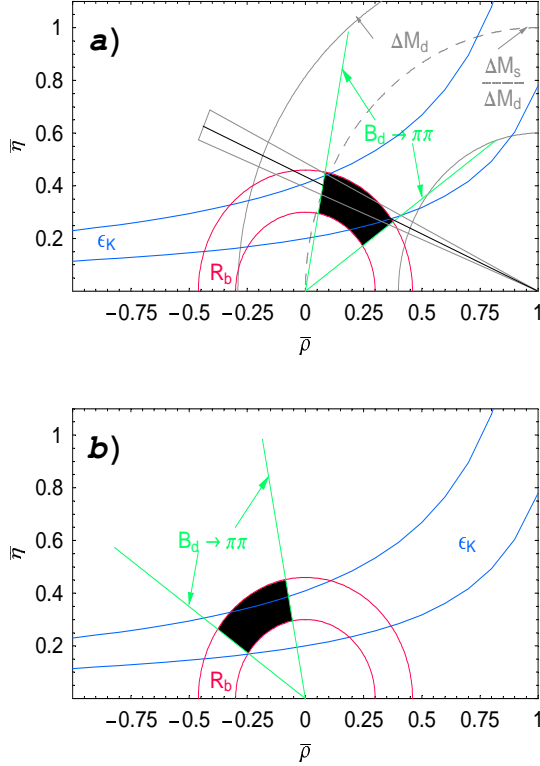


**Figure 3.** The allowed regions for the UT fixed through  $R_b$  and CP violation in  $B_d \rightarrow \pi^+ \pi^-$ , as described in the text: (a) and (b) correspond to  $\phi_d = 47^\circ$  and  $\phi_d = 133^\circ$ , respectively ( $H = 7.5$ ).

CP-averaged branching ratios, plays a key rôle:

$$H = \frac{1}{\epsilon} \left( \frac{f_K}{f_\pi} \right)^2 \left[ \frac{\text{BR}(B_d \rightarrow \pi^+ \pi^-)}{\text{BR}(B_d \rightarrow \pi^\mp K^\pm)} \right], \quad (17)$$

where  $\epsilon \equiv \lambda^2/(1 - \lambda^2)$ . The current experimental status of  $H$  is given by

$$H = \begin{cases} 7.4 \pm 2.5 & (\text{CLEO [18]}) \\ 7.8 \pm 1.2 & (\text{BaBar [19]}) \\ 7.1 \pm 1.2 & (\text{Belle [19]}). \end{cases} \quad (18)$$

If we apply (16), we may write

$$H = \text{fct}(d, \theta, \gamma). \quad (19)$$

Consequently, (14) and (19) provide sufficient information to determine  $\gamma$ ,  $d$  and  $\theta$  [24, 25]. As discussed in detail in [17], if we follow these lines and complement the twofold solution  $\phi_d \sim 47^\circ \vee 133^\circ$ , which is implied by the measured mixing-induced CP violation in  $B_d \rightarrow J/\psi K_S$ , with (11), (12) and (18), we obtain the following picture: in the case of  $\phi_d = 47^\circ$ , the data point towards  $\gamma \sim 60^\circ$ , so that not only  $\phi_d$  would be in accordance with the CKM fits, but also  $\gamma$ . On the other hand, for  $\phi_d = 133^\circ$ , the experimental values favour  $\gamma \sim 120^\circ$ . At first sight, this may look

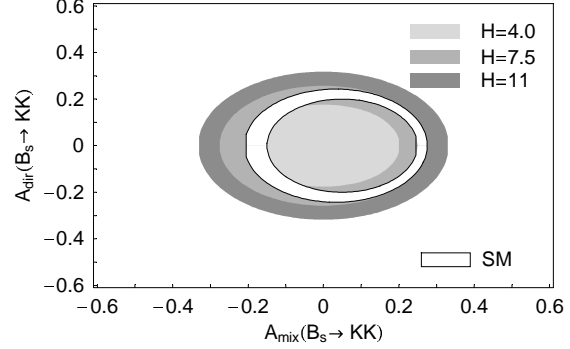


**Figure 4.** The allowed regions in the  $B_s \rightarrow K^+ K^-$  observable space originating for  $\phi_s = 0^\circ$  and for various values of  $H$ . The SM region appears if we restrict  $\gamma$  to (4) and choose  $H = 7.5$ .

puzzling. However, since the  $\phi_d = 133^\circ$  solution would definitely require NP contributions to  $B_d^0 - \bar{B}_d^0$  mixing, we may no longer use the SM interpretation of  $\Delta M_d$  in this case to fix the UT side  $R_t$ , which is a crucial ingredient for the  $\gamma$  range in (4). Consequently, if we choose  $\phi_d = 133^\circ$ ,  $\gamma$  may well be larger than  $90^\circ$ . As we have already noted, the  $B \rightarrow \pi K$  data seem to favour such values; a similar feature is also suggested by the observed small  $B_d \rightarrow \pi^+ \pi^-$  rate [17, 25]. Interestingly, the measured branching ratio for the rare kaon decay  $K^+ \rightarrow \pi^+ \nu \bar{\nu}$  seems to point towards  $\gamma > 90^\circ$  as well [34, 35], thereby also favouring the unconventional solution of  $\phi_d = 133^\circ$  [36]. Further valuable information on this exciting possibility can be obtained in the future from the rare decays  $B_{s,d} \rightarrow \mu^+ \mu^-$ .

We could straightforwardly accommodate this picture in a NP scenario, where we have large effects in  $B_d^0 - \bar{B}_d^0$  mixing, but not in the  $\Delta B = 1$  and  $\Delta S = 1$  decay processes. Such kind of NP was already considered several years ago [37, 38], and can be motivated by generic arguments and within supersymmetry [36]. Since the determination of  $R_b$  through semileptonic tree decays is in general very robust under NP effects and would not be affected either in this particular scenario, we may complement  $R_b$  with the range for  $\gamma$  extracted from our  $B_d \rightarrow \pi^+ \pi^-$  analysis, allowing us to fix the apex of the UT in the  $\bar{\rho} - \bar{\eta}$  plane. The results of this exercise are summarized in Fig. 3, following [36], where also numerical values for  $\alpha$ ,  $\beta$  and  $\gamma$  are given and a detailed discussion of the theoretical uncertainties can be found (see also [39]). Note that the SM contours implied by  $\Delta M_d$ , which are included in Fig. 3 (a) to guide the eye, are absent in (b) since, there,  $B_d^0 - \bar{B}_d^0$  mixing would receive NP contributions. In this case also, we may no longer simply represent  $\phi_d$  by a straight line, as the one in Fig. 3 (a), which corresponds to  $\phi_d^{\text{SM}} = 2\beta$ , since we would now have  $\phi_d = 2\beta + \phi_d^{\text{NP}}$ , with  $\phi_d^{\text{NP}} \neq 0^\circ$ . However, we may easily read off the “correct” value of  $\beta$  from the black region in Fig. 3 (b) [36]. Interestingly, both black regions in Fig. 3 (a) and (b) are consistent with the SM  $\epsilon_K$  hyperbola.

Since the current experimental status of the CP-violating  $B_d \rightarrow \pi^+\pi^-$  observables is unsatisfactory, we may not yet draw definite conclusions from this analysis, although it illustrates nicely how the corresponding strategy works. However, the  $B$ -factory measurements of CP violation in  $B_d \rightarrow \pi^+\pi^-$  will improve significantly in the future, thereby providing more stringent constraints on  $\gamma$ , which we may then convert into narrower ranges for the apex of the UT. Another milestone in this programme is the measurement of the CP-averaged  $B_s \rightarrow K^+K^-$  branching ratio at run II of the Tevatron, which will allow a much better determination of  $H$  that no longer relies on dynamical assumptions. Finally, if also the direct and mixing-induced CP asymmetries of  $B_s \rightarrow K^+K^-$  are measured, we may determine  $\gamma$  through a minimal  $U$ -spin input, as we have sketched above. Interestingly,  $H$  implies already a very narrow SM target region in the space of the CP-violating  $B_s \rightarrow K^+K^-$  observables, as can be seen in Fig. 4. It will be exciting to see whether the data will actually fall into the small elliptical region in this figure. After important steps by the CDF collaboration, LHCb and BTeV should be able to fully exploit the rich physics potential of the  $B_d \rightarrow \pi^+\pi^-$ ,  $B_s \rightarrow K^+K^-$  system.

There are several other promising  $B_s$  decays, which we shall address in the discussion of the following section.

### 3 Theoretically Clean Strategies

In order to determine  $\gamma$  in a theoretically clean manner, pure tree decays of  $B$  mesons play the central rôle. There are basically two kinds of approaches:

- i We may induce interference effects in  $B$  decays through subsequent decays of neutral  $D$  mesons, satisfying  $D^0, \bar{D}^0 \rightarrow f_D$ . Important examples are  $B^\pm \rightarrow DK^\pm$ ,  $B_c^\pm \rightarrow DD_s^\pm$ , ... modes [40]–[45].
- ii We may employ neutral  $B_q$  modes, where both  $B_q^0$  and  $\bar{B}_q^0$  may decay into the same final state, yielding interference between mixing and decay processes, e.g.  $B_d \rightarrow D^{(*)\pm}\pi^\mp$ ,  $B_s \rightarrow D_s^{(*)\pm}K^\mp$ , ... [46]–[50].

In this section, we will focus on two kinds of new strategies, which were proposed in [51, 52] and [53].

#### 3.1 $B_d \rightarrow DK_{S(L)}$ , $B_s \rightarrow D\eta^{(\prime)}$ , $D\phi$ , ...

Colour-suppressed  $B_d^0 \rightarrow D^0 K_S$  decays and similar modes provide interesting tools to explore CP violation [54, 55]. In the following, we consider  $B_q^0 \rightarrow D^0 f_r$  transitions, where  $r \in \{s, d\}$  distinguishes between  $b \rightarrow Ds$  and  $b \rightarrow Dd$  processes [51, 52]. If we require  $(\mathcal{CP})|f_r\rangle = \eta_{\mathcal{CP}}^f |f_r\rangle$ ,  $B_q^0$  and  $\bar{B}_q^0$  mesons may both decay into  $D^0 f_r$ , thereby leading to interference effects between  $B_q^0$ – $\bar{B}_q^0$  mixing and decay processes, which involve the weak phase  $\phi_q + \gamma$  (see ii):

- For  $r = s$ , i.e.  $B_d \rightarrow DK_{S(L)}$ ,  $B_s \rightarrow D\eta^{(\prime)}$ ,  $D\phi$ , ... modes, these interference effects are governed by a hadronic parameter  $x_{fs} e^{i\delta_{fs}} \propto R_b \approx 0.4$ , and are hence favourably large.
- For  $r = d$ , i.e.  $B_s \rightarrow DK_{S(L)}$ ,  $B_d \rightarrow D\pi^0$ ,  $D\rho^0$  ... modes, the interference effects are tiny because of  $x_{fd} e^{i\delta_{fd}} \propto -\lambda^2 R_b \approx -0.02$ .

Let us first focus on the  $r = s$  case. If we consider  $B_q \rightarrow D_\pm f_s$  modes, where  $(\mathcal{CP})|D_\pm\rangle = \pm|D_\pm\rangle$ , additional interference effects between  $B_q^0 \rightarrow D^0 f_s$  and  $B_q^0 \rightarrow \bar{D}^0 f_s$  arise at the decay level, involving  $\gamma$  (see i). The most straightforward observable is the “untagged” rate

$$\begin{aligned} \langle \Gamma(B_q(t) \rightarrow D_\pm f_s) \rangle &\equiv \Gamma(B_q^0(t) \rightarrow D_\pm f_s) + \Gamma(\bar{B}_q^0(t) \rightarrow D_\pm f_s) \\ &\stackrel{\Delta\Gamma_q=0}{=} \left[ \Gamma(B_q^0 \rightarrow D_\pm f_s) + \Gamma(\bar{B}_q^0 \rightarrow D_\pm f_s) \right] e^{-\Gamma_q t} \\ &\equiv \langle \Gamma(B_q \rightarrow D_\pm f_s) \rangle e^{-\Gamma_q t}, \end{aligned} \quad (20)$$

providing the following “untagged” rate asymmetry:

$$\Gamma_{+-}^{f_s} \equiv \frac{\langle \Gamma(B_q \rightarrow D_+ f_s) \rangle - \langle \Gamma(B_q \rightarrow D_- f_s) \rangle}{\langle \Gamma(B_q \rightarrow D_+ f_s) \rangle + \langle \Gamma(B_q \rightarrow D_- f_s) \rangle}. \quad (21)$$

Interestingly, already the quantity  $\Gamma_{+-}^{f_s}$  offers valuable information about  $\gamma$  [51], since bounds on this angle are implied by

$$|\cos \gamma| \geq |\Gamma_{+-}^{f_s}|. \quad (22)$$

Moreover, if we take into account that the factorization picture suggests  $\cos \delta_{fs} > 0$  [52], we obtain

$$\text{sgn}(\cos \gamma) = \text{sgn}(\Gamma_{+-}^{f_s}), \quad (23)$$

i.e. we may decide whether  $\gamma$  is smaller or larger than  $90^\circ$ . If we employ, in addition, the mixing-induced observables  $S_\pm^{f_s} \equiv \mathcal{A}_{\mathcal{CP}}^{\text{mix}}(B_q \rightarrow D_\pm f_s)$ , we may determine  $\gamma$ . To this end, it is convenient to introduce the quantities

$$\langle S_{f_s} \rangle_\pm \equiv (S_+^{f_s} \pm S_-^{f_s})/2. \quad (24)$$

Expressing the  $\langle S_{f_s} \rangle_\pm$  in terms of the  $B_q \rightarrow D_\pm f_s$  decay parameters gives rather complicated formulae. However, complementing the  $\langle S_{f_s} \rangle_\pm$  with  $\Gamma_{+-}^{f_s}$  yields

$$\tan \gamma \cos \phi_q = \left[ \frac{\eta_{f_s} \langle S_{f_s} \rangle_+}{\Gamma_{+-}^{f_s}} \right] + [\eta_{f_s} \langle S_{f_s} \rangle_- - \sin \phi_q], \quad (25)$$

where  $\eta_{f_s} \equiv (-1)^L \eta_{\mathcal{CP}}^{f_s}$ , with  $L$  denoting the  $Df_s$  angular momentum [51]. Using this simple – but *exact* – relation, we obtain the twofold solution  $\gamma = \gamma_1 \vee \gamma_2$ , with

$\gamma_1 \in [0^\circ, 180^\circ]$  and  $\gamma_2 = \gamma_1 + 180^\circ$ . Since  $\cos \gamma_1$  and  $\cos \gamma_2$  have opposite signs, (23) allows us to fix  $\gamma$  *unambiguously*. Another advantage of (25) is that  $\langle S_{f_s} \rangle_+$  and  $\Gamma_{+-}^{f_s}$  are both proportional to  $x_{f_s} \approx 0.4$ , so that the first term in square brackets is of  $O(1)$ , whereas the second one is of  $O(x_{f_s}^2)$ , hence playing a minor rôle. In order to extract  $\gamma$ , we may also employ  $D$  decays into CP non-eigenstates  $f_{\text{NE}}$ , where we have to deal with complications originating from  $D^0, \bar{D}^0 \rightarrow f_{\text{NE}}$  interference effects [55]. Also in this case,  $\Gamma_{+-}^{f_s}$  is a very powerful ingredient, offering an efficient, *analytical* strategy to include these interference effects in the extraction of  $\gamma$  [52].

Let us now briefly come back to the  $r = d$  case, corresponding to  $B_s \rightarrow DK_{S(L)}$ ,  $B_d \rightarrow D\pi^0, D\rho^0 \dots$  decays, which can be described through the same formulae as their  $r = s$  counterparts. Since the relevant interference effects are governed by  $x_{fd} \approx -0.02$ , these channels are not as attractive for the extraction of  $\gamma$  as the  $r = s$  modes. On the other hand, the relation

$$\eta_{fd} \langle S_{fd} \rangle_- = \sin \phi_q + O(x_{fd}^2) = \sin \phi_q + O(4 \times 10^{-4}) \quad (26)$$

offers very interesting determinations of  $\sin \phi_q$  [51]. Following this avenue, there are no penguin uncertainties, and the theoretical accuracy is one order of magnitude better than in the “conventional”  $B_d \rightarrow J/\psi K_S$ ,  $B_s \rightarrow J/\psi \phi$  strategies. In particular,  $\phi_s^{\text{SM}} = -2\lambda^2 \eta$  could, in principle, be determined with a theoretical uncertainty of only  $O(1\%)$ , in contrast to the extraction from the  $B_s \rightarrow J/\psi \phi$  angular distribution, which suffers from generic penguin uncertainties at the 10% level.

Let us finally note that  $\bar{B}_d^0 \rightarrow D^0 \pi^0$  has already been measured at the  $B$  factories, with branching ratios at the  $3 \times 10^{-4}$  level [56]. Interestingly, the Belle collaboration has recently announced the observation of  $\bar{B}_d^0 \rightarrow D^0 \bar{K}^0$ , with the branching ratio  $(5.0_{-1.2}^{+1.3} \pm 0.6) \times 10^{-5}$  [57].

### 3.2 $B_s \rightarrow D_s^{(*)\pm} K^\mp, \dots$ and $B_d \rightarrow D^{(*)\pm} \pi^\mp, \dots$

Let us now consider the colour-allowed counterparts of the  $B_q \rightarrow Df_q$  modes discussed above, which we may write generically as  $B_q \rightarrow D_q \bar{u}_q$  [53]. The characteristic feature of these transitions is that both a  $B_q^0$  and a  $\bar{B}_q^0$  meson may decay into  $D_q \bar{u}_q$ , thereby leading to interference between  $B_q^0$ – $\bar{B}_q^0$  mixing and decay processes, which involve the weak phase  $\phi_q + \gamma$  (see ii):

- In the case of  $q = s$ , i.e.  $D_s \in \{D_s^+, D_s^{*+}, \dots\}$  and  $u_s \in \{K^+, K^{*+}, \dots\}$ , these interference effects are governed by a hadronic parameter  $x_s e^{i\delta_s} \propto R_b \approx 0.4$ , and hence are large.
- In the case of  $q = d$ , i.e.  $D_d \in \{D^+, D^{*+}, \dots\}$  and  $u_d \in \{\pi^+, \rho^+, \dots\}$ , the interference effects are described by  $x_d e^{i\delta_d} \propto -\lambda^2 R_b \approx -0.02$ , and hence are tiny.

In the following, we shall only consider  $B_q \rightarrow D_q \bar{u}_q$  modes, where at least one of the  $D_q, \bar{u}_q$  states is a pseudoscalar meson; otherwise a complicated angular analysis has to be performed [58]–[60].

It is well known that such decays allow a determination of  $\phi_q + \gamma$ , where the “conventional” approach works as follows [46]–[50]: if we measure the observables  $C(B_q \rightarrow D_q \bar{u}_q) \equiv C_q$  and  $C(B_q \rightarrow \bar{D}_q u_q) \equiv \bar{C}_q$  provided by the  $\cos(\Delta M_q t)$  pieces of the time-dependent rate asymmetries, we may determine  $x_q$  from terms entering at the  $x_q^2$  level. In the case of  $q = s$ , we have  $x_s = O(R_b)$ , implying  $x_s^2 = O(0.16)$ , so that this may actually be possible, though challenging. On the other hand,  $x_d = O(-\lambda^2 R_b)$  is doubly Cabibbo-suppressed. Although it should be possible to resolve terms of  $O(x_d)$ , this will be impossible for the vanishingly small  $x_d^2 = O(0.0004)$  terms, so that other approaches to fix  $x_d$  are required [46]–[49]. In order to extract  $\phi_q + \gamma$ , the mixing-induced observables  $S(B_q \rightarrow D_q \bar{u}_q) \equiv S_q$  and  $S(B_q \rightarrow \bar{D}_q u_q) \equiv \bar{S}_q$  associated with the  $\sin(\Delta M_q t)$  terms of the time-dependent rate asymmetries must be measured, where it is convenient to introduce

$$\langle S_q \rangle_\pm \equiv (\bar{S}_q \pm S_q) / 2. \quad (27)$$

If we assume that  $x_q$  is known, we may consider

$$s_+ \equiv (-1)^L \left[ \frac{1 + x_q^2}{2x_q} \right] \langle S_q \rangle_+ = +\cos \delta_q \sin(\phi_q + \gamma) \quad (28)$$

$$s_- \equiv (-1)^L \left[ \frac{1 + x_q^2}{2x_q} \right] \langle S_q \rangle_- = -\sin \delta_q \cos(\phi_q + \gamma), \quad (29)$$

yielding

$$\sin^2(\phi_q + \gamma) = \frac{1 + s_+^2 - s_-^2}{2} \pm \sqrt{\frac{(1 + s_+^2 - s_-^2)^2 - 4s_+^2}{4}}, \quad (30)$$

which implies an eightfold solution for  $\phi_q + \gamma$ . If we assume that  $\text{sgn}(\cos \delta_q) > 0$ , as suggested by factorization, a fourfold discrete ambiguity emerges. Note that this assumption allows us also to extract the sign of  $\sin(\phi_q + \gamma)$  from  $\langle S_q \rangle_+$ . To this end, the factor  $(-1)^L$ , where  $L$  is the  $D_q \bar{u}_q$  angular momentum, has to be properly taken into account [53]. This is crucial for the extraction of the sign of  $\sin(\phi_d + \gamma)$  from  $B_d \rightarrow D^{*\pm} \pi^\mp$  modes, allowing us to distinguish between the two solutions shown in Fig. 3.

Let us now discuss new strategies to exploit the interesting physics potential of the  $B_q \rightarrow D_q \bar{u}_q$  modes, following [53]. If the width difference  $\Delta\Gamma_s$  of the  $B_s$  mass eigenstates is sizeable, the “untagged” rates

$$\begin{aligned} \langle \Gamma(B_q(t) \rightarrow D_q \bar{u}_q) \rangle &= \langle \Gamma(B_q \rightarrow D_q \bar{u}_q) \rangle e^{-\Gamma_q t} \\ &\times \left[ \cosh(\Delta\Gamma_q t / 2) - \mathcal{A}_{\Delta\Gamma}(B_q \rightarrow D_q \bar{u}_q) \sinh(\Delta\Gamma_q t / 2) \right] \end{aligned} \quad (31)$$



and their CP conjugates provide observables  $\mathcal{A}_{\Delta\Gamma}(B_s \rightarrow D_s \bar{u}_s) \equiv \mathcal{A}_{\Delta\Gamma_s}$  and  $\mathcal{A}_{\Delta\Gamma}(B_s \rightarrow \bar{D}_s u_s) \equiv \bar{\mathcal{A}}_{\Delta\Gamma_s}$ , which yield

$$\tan(\phi_s + \gamma) = - \left[ \frac{\langle S_s \rangle_+}{\langle \mathcal{A}_{\Delta\Gamma_s} \rangle_+} \right] = + \left[ \frac{\langle \mathcal{A}_{\Delta\Gamma_s} \rangle_-}{\langle S_s \rangle_-} \right], \quad (32)$$

where the  $\langle \mathcal{A}_{\Delta\Gamma_s} \rangle_{\pm}$  are defined in analogy to (27). These relations allow an *unambiguous* extraction of  $\phi_s + \gamma$ , if we employ again  $\text{sgn}(\cos \delta_q) > 0$ . Another important advantage of (32) is that we do *not* have to rely on  $O(x_s^2)$  terms, as  $\langle S_s \rangle_{\pm}$  and  $\langle \mathcal{A}_{\Delta\Gamma_s} \rangle_{\pm}$  are proportional to  $x_s$ . On the other hand, we need a sizeable value of  $\Delta\Gamma_s$ . Measurements of untagged rates are also very useful in the case of vanishingly small  $\Delta\Gamma_q$ , since the “unevolved” untagged rates in (31) offer various interesting strategies to determine  $x_q$  from the ratio of  $\langle \Gamma(B_q \rightarrow D_q \bar{u}_q) \rangle + \langle \Gamma(B_q \rightarrow \bar{D}_q u_q) \rangle$  and CP-averaged rates of appropriate  $B^{\pm}$  or flavour-specific  $B_q$  decays.

If we keep the hadronic parameter  $x_q$  and the associated strong phase  $\delta_q$  as “unknown”, free parameters in the expressions for the  $\langle S_q \rangle_{\pm}$ , we obtain

$$|\sin(\phi_q + \gamma)| \geq |\langle S_q \rangle_+|, \quad |\cos(\phi_q + \gamma)| \geq |\langle S_q \rangle_-|, \quad (33)$$

which can straightforwardly be converted into bounds on  $\phi_q + \gamma$ . If  $x_q$  is known, stronger constraints are implied by

$$|\sin(\phi_q + \gamma)| \geq |s_+|, \quad |\cos(\phi_q + \gamma)| \geq |s_-|. \quad (34)$$

Once  $s_+$  and  $s_-$  are known, we may of course determine  $\phi_q + \gamma$  through the “conventional” approach, using (30). However, the bounds following from (34) provide essentially the same information and are much simpler to implement. Moreover, as discussed in detail in [53] for several examples, the bounds following from  $B_s$  and  $B_d$  modes may be highly complementary, thereby providing particularly narrow, theoretically clean ranges for  $\gamma$ .

Let us now further exploit the complementarity between  $B_s^0 \rightarrow D_s^{(*)+} K^-$  and  $B_d^0 \rightarrow D^{(*)+} \pi^-$  modes. If we look at the corresponding decay topologies, we observe that these channels are related to each other through an interchange of all down and strange quarks. Consequently, the  $U$ -spin symmetry implies  $a_s = a_d$  and  $\delta_s = \delta_d$ , where  $a_s = x_s/R_b$  and  $a_d = -x_d/(\lambda^2 R_b)$  are the ratios of hadronic matrix elements entering  $x_s$  and  $x_d$ , respectively. There are various possibilities to implement these relations [53]. A particularly simple picture emerges if we assume that  $a_s = a_d$  and  $\delta_s = \delta_d$ , which yields

$$\tan \gamma = - \left[ \frac{\sin \phi_d - S \sin \phi_s}{\cos \phi_d - S \cos \phi_s} \right]_{\phi_s=0^\circ} = - \left[ \frac{\sin \phi_d}{\cos \phi_d - S} \right]. \quad (35)$$

Here we have introduced

$$S = -R \left[ \frac{\langle S_d \rangle_+}{\langle S_s \rangle_+} \right] \quad (36)$$

with

$$R = \left( \frac{1 - \lambda^2}{\lambda^2} \right) \left[ \frac{1}{1 + x_s^2} \right], \quad (37)$$

where  $R$  can be fixed from untagged  $B_s$  rates through

$$R = \left( \frac{f_K}{f_\pi} \right)^2 \frac{\Gamma(\bar{B}_s^0 \rightarrow D_s^{(*)+} \pi^-) + \Gamma(B_s^0 \rightarrow D_s^{(*)-} \pi^+)}{\langle \Gamma(B_s \rightarrow D_s^{(*)+} K^-) \rangle + \langle \Gamma(B_s \rightarrow D_s^{(*)-} K^+) \rangle}. \quad (38)$$

Alternatively, we may *only* assume that  $\delta_s = \delta_d$  or that  $a_s = a_d$ , as discussed in detail in [53]. Apart from features related to multiple discrete ambiguities, the most important advantage with respect to the “conventional” approach is that the experimental resolution of the  $x_q^2$  terms is not required. In particular,  $x_d$  does *not* have to be fixed, and  $x_s$  may only enter through a  $1 + x_s^2$  correction, which can straightforwardly be determined through untagged  $B_s$  rate measurements. In the most refined implementation of this strategy, the measurement of  $x_d/x_s$  would *only* be interesting for the inclusion of  $U$ -spin-breaking effects in  $a_d/a_s$ . Moreover, we may obtain interesting insights into hadron dynamics and  $U$ -spin-breaking effects.

## 4 Conclusions and Outlook

In order to perform stringent tests of the SM description of CP violation, it is essential to determine the angle  $\gamma$  of the UT in a variety of ways. We may divide the corresponding strategies into methods employing the flavour symmetries of strong interactions and theoretically clean approaches.

As far as the former avenue is concerned,  $B \rightarrow \pi K$  decays are an important representative. Interestingly, the  $B$ -factory data both for the charged and for the neutral  $B \rightarrow \pi K$  modes point separately towards  $\gamma \gtrsim 90^\circ$ , which would be larger than the typical range following from the CKM fits. On the other hand, the data favour also conflicting ranges for the corresponding strong phases, so that we arrive at a puzzling picture. The experimental uncertainties do not yet allow us to draw definite conclusions, but the situation will improve in the future. A particularly promising strategy for  $B$ -decay experiments at hadron colliders is offered by  $B_s \rightarrow K^+ K^-$ , which complements  $B_d \rightarrow \pi^+ \pi^-$  nicely, thereby allowing the determination of  $\gamma$  with the help of a “minimal”  $U$ -spin input. Since  $B_s \rightarrow K^+ K^-$  is not accessible at the  $e^+ e^-$   $B$  factories operating at  $\Upsilon(4S)$ , we may not yet confront this strategy with data. However, we may approximately replace  $B_s \rightarrow K^+ K^-$  by  $B_d \rightarrow \pi^+ \pi^-$  to deal with the penguin effects in  $B_d \rightarrow \pi^+ \pi^-$ . Interestingly, the analysis of the corresponding data suggests that we may accommodate  $\gamma > 90^\circ$  for the “unconventional” solution  $\phi_d = 133^\circ$  of the  $B_d^0 - \bar{B}_d^0$  mixing phase, whereas we obtain a picture in accordance with the SM for  $\phi_d = 47^\circ$ .

In our discussion of theoretically clean strategies, we have focused on two new approaches: first, we have seen that  $B_d \rightarrow DK_{S(L)}$ ,  $B_s \rightarrow D\eta^{(\prime)}, D\phi$ , ... modes provide efficient and unambiguous extractions of  $\tan \gamma$  if we combine an “untagged” rate asymmetry with mixing-induced observables. On the other hand, the  $B_s \rightarrow D_{\pm}K_{S(L)}$ ,  $B_d \rightarrow D_{\pm}\pi^0, D_{\pm}\rho^0$ , ... counterparts of these decays are not as attractive for the determination of  $\gamma$ , but allow extremely clean extractions of  $\sin \phi_s$  and  $\sin \phi_d$ , which may be particularly interesting for the  $\phi_s$  case. Second, we have discussed interesting new aspects of  $B_s \rightarrow D_s^{(*)\pm}K^{\mp}$ , ... and  $B_d \rightarrow D^{(*)\pm}\pi^{\mp}$ , ... decays. The observables of these modes provide clean bounds on  $\phi_q + \gamma$ , where the resulting ranges for  $\gamma$  may be highly complementary in the  $B_s$  and  $B_d$  cases, thereby yielding stringent constraints on  $\gamma$ . Moreover, it is of great advantage to combine the  $B_d \rightarrow D^{(*)\pm}\pi^{\mp}$  modes with their  $U$ -spin counterparts  $B_s \rightarrow D_s^{(*)\pm}K^{\mp}$ , allowing us to overcome the main problems of the “conventional” strategies to deal with these modes. We strongly encourage detailed feasibility studies of these new strategies.

## References

1. M Battaglia, AJ Buras, P Gambino and A Stocchi, eds. Proceedings of the *First Workshop on the CKM Unitarity Triangle*, CERN, Feb 2002, hep-ph/0304132
2. L Wolfenstein, *Phys. Rev. Lett.* **51** (1983) 1945
3. AJ Buras *et al.*, *Phys. Rev.* **D50** (1994) 3433
4. R Fleischer, *Phys. Rep.* **370** (2002) 537
5. R Fleischer, *Phys. Lett.* **B365** (1996) 399
6. R Fleischer, T Mannel, *Phys. Rev.* **D57** (1998) 2752
7. M Gronau, JL Rosner, *Phys. Rev.* **D57** (1998) 6843
8. R Fleischer, *Eur. Phys. J.* **C6** (1999) 451; *Phys. Lett.* **B435** (1998) 221
9. M Neubert, JL Rosner, *Phys. Lett.* **B441** (1998) 403; *Phys. Rev. Lett.* **81** (1998) 5076
10. M Neubert, *JHEP* **9902** (1999) 014
11. AJ Buras and R Fleischer, *Eur. Phys. J.* **C11** (1999) 93
12. AJ Buras and R Fleischer, *Eur. Phys. J.* **C16** (2000) 97
13. M Beneke *et al.*, *Phys. Rev. Lett.* **83** (1999) 1914
14. M Beneke *et al.*, *Nucl. Phys.* **B606** (2001) 245
15. M Gronau, JL Rosner and D London, *Phys. Rev. Lett.* **73** (1994) 21
16. R Fleischer, J Matias, *Phys. Rev.* **D61** (2000) 074004
17. R Fleischer, J Matias, *Phys. Rev.* **D66** (2002) 054009
18. A Bornheim *et al.* (CLEO Collaboration), CLEO-03-03 [hep-ex/0302026]
19. J Olsen, these proceedings
20. AI Sanda, K Ukai, *Prog. Theor. Phys.* **107** (2002) 421; YY Keum, DPNU-02-30 [hep-ph/0209208].
21. J Matias, *Phys. Lett.* **B520** (2001) 131
22. M Bargiotti *et al.*, *Eur. Phys. J.* **C24** (2002) 361
23. M Gronau, JL Rosner, *Phys. Rev.* **D65** (2002), 013004 [E: **D65** (2002) 079901]
24. R Fleischer, *Phys. Lett.* **B459** (1999) 306
25. R Fleischer, *Eur. Phys. J.* **C16** (2000) 87
26. B Aubert *et al.* (BaBar Collaboration), *Phys. Rev. Lett.* **89** (2002) 281802
27. K Abe *et al.* (Belle Collaboration), Belle preprint 2003-1 [hep-ex/0301032]
28. Particle Data Group (K. Hagiwara *et al.*), *Phys. Rev.* **D66** (2002) 010001
29. K Anikeev *et al.*, hep-ph/0201071
30. P Ball *et al.*, CERN-TH/2000-101 [hep-ph/0003238], in CERN Report on *Standard Model physics (and more) at the LHC* (CERN, Geneva, 2000) p. 305
31. V Vagnoni, these proceedings
32. M Beneke, these proceedings
33. JP Silva, L Wolfenstein, *Phys. Rev.* **D49** (1994) 1151
34. G D’Ambrosio and G Isidori, *Phys. Lett.* **B530** (2002) 108
35. G Isidori, these proceedings
36. R Fleischer, G Isidori and J Matias, *JHEP* **0305** (2003) 053
37. Y Grossman, Y Nir and M Worah, *Phys. Lett.* **B407** (1997) 307
38. J Silva, L Wolfenstein, *Phys. Rev.* **D62** (2000) 014018
39. J Matias, these proceedings [hep-ph/0306058]
40. M Gronau, D Wyler, *Phys. Lett.* **B265** (1991) 172
41. D Atwood *et al.*, *Phys. Rev.* **D63** (2001) 036005
42. R Fleischer, D Wyler, *Phys. Rev.* **D62** (2000) 057503
43. R Aleksan *et al.*, *Phys. Rev.* **D67** (2003) 096002
44. Y Grossman *et al.*, *Phys. Rev.* **D67** (2003) 071301
45. M Gronau, *Phys. Lett.* **B557** (2003) 198
46. I Dunietz and RG Sachs, *Phys. Rev.* **D37** (1988) 3186 [E: **D39** (1989) 3515]
47. I Dunietz, *Phys. Lett.* **B427** (1998) 179
48. M Diehl and G Hiller, *Phys. Lett.* **B517** (2001) 125
49. DA Suprun *et al.*, *Phys. Rev.* **D65** (2002) 054025
50. R Aleksan *et al.*, *Z. Phys.* **C54** (1992) 653
51. R Fleischer, *Phys. Lett.* **B562** (2003) 234
52. R Fleischer, *Nucl. Phys.* **B659** (2003) 321
53. R Fleischer, CERN-TH/2003-084 [hep-ph/0304027].
54. M Gronau, D London., *Phys. Lett.* **B253** (1991) 483
55. B Kayser, D London, *Phys. Rev.* **D61** (2000) 116013
56. K Abe *et al.* (Belle Collaboration), *Phys. Rev. Lett.* **88** (2002) 052002; TE Coan *et al.* (CLEO Collaboration), *Phys. Rev. Lett.* **88** (2002) 062001; B Aubert *et al.* (BaBar Collaboration), BABAR-CONF-02/17 [hep-ex/0207092].
57. P Krokovny *et al.* (Belle Collaboration), *Phys. Rev. Lett.* **90** (2003) 141802
58. R Fleischer, I Dunietz, *Phys. Lett.* **B387** (1996) 361
59. D London *et al.*, *Phys. Rev. Lett.* **85** (2000) 1807
60. M Gronau *et al.*, *Phys. Rev. Lett.* **90** (2003) 051801